IEEE Photonics Journal
An IEEE Photonics Society Publication

Open Access

Lumped Time-Delay Compensation Scheme for Coding Synchronization in the Nonlinear Spectral Quantization-Based All-Optical Analog-to-Digital Conversion

Volume 5, Number 6, December 2013

Zhe Kang
Jinhui Yuan
Qiang Wu
Tao Wang
Sha Li
Xinzhu Sang
Chongxiu Yu
Gerald Farrell

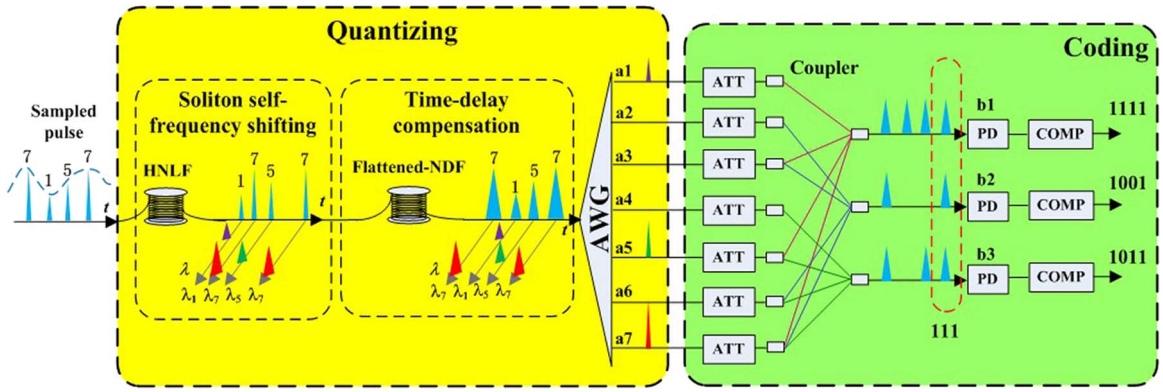

DOI: 10.1109/JPHOT.2013.2284252
1943-0655 © 2013 IEEE

Lumped Time-Delay Compensation Scheme for Coding Synchronization in the Nonlinear Spectral Quantization-Based All-Optical Analog-to-Digital Conversion

Zhe Kang,[1] Jinhui Yuan,[1,2] Qiang Wu,[1,3] Tao Wang,[1] Sha Li,[1] Xinzhu Sang,[1] Chongxiu Yu,[1] and Gerald Farrell[3]

[1]State Key Laboratory of Information Photonics and Optical Communications, Beijing University of Posts and Telecommunications (BUPT), Beijing 100876, China
[2]Laboratory of Nanophotonic Functional Materials and Devices, South China Normal University, Guangzhou 510006, China
[3]Photonics Research Center, Dublin Institute of Technology, Dublin, Ireland

DOI: 10.1109/JPHOT.2013.2284252
1943-0655 © 2013 IEEE

Manuscript received September 8, 2013; revised September 24, 2013; accepted September 26, 2013. Date of publication October 2, 2013; date of current version November 21, 2013. This work was supported in part by the National Basic Research Program under Grants 2010CB327605 and 2010CB328304, by the National High-Technology Research and Development Program of China under Grant 2013AA031501, by the National Natural Science Foundation of China under Grant 61307109, by the Ministry of Education under Key Grant 109015, by the Program for New Century Excellent Talents in University under Grant NECT-11-0596, by the Beijing Nova Program under Grant 2011066, by the Specialized Research Fund for the Doctoral Program of Higher Education under Grant 20120005120021, by the Fundamental Research Funds for the Central Universities under Grant 2013RC1202, by the China Postdoctoral Science Foundation under Grant 2012M511826, by the Postdoctoral Science Foundation of Guangdong Province under Grant 244331, and by the Science Foundation Ireland under Grants SFI/12/ISCA/2496, 07/SK/I1200, 11/TIDA/B2051, 07/SK/I1200-STTF11, and DT900/1. Corresponding authors: Z. Kang and J. Yuan (e-mail: kangtony9999@163.com; yuanjinhui81@163.com).

Abstract: In this paper, we propose a novel lumped time-delay compensation scheme for the all-optical analog-to-digital conversion based on soliton self-frequency shift and optical interconnection techniques. By inserting a segment of negative dispersion fiber between the quantization and the coding module, the time delay of different quantized pulses can be accurately compensated with a simple structure compared to the multiple time-delay lines. The simulation results show that the coding pulses can be well synchronized using a span of fiber, with the flattened negative dispersion within the wavelength range of 1558–1620 nm. In addition, the problems of pulse broadening and time error are discussed, and it is shown that no damage happens to the coding correctness within the sampling rate of 30 GSa/s.

Index Terms: All-optical analog-to-digital, lumped time-delay compensation, negative dispersion fiber, soliton self-frequency shift.

1. Introduction

With the rapid development of ultra-fast signal processing in the high speed optical communication, advanced radar system and real-time signal monitoring, the requirements of high performance analog-to-digital converter (ADC) become very urgent [1], [2]. "Photonic ADCs" is an efficient technology to overcome the inherent jitter of the sampling aperture and ambiguity of the comparator in the electronic devices and has achieved lots of developments since the early 1970s [1]–[3]. Jalali *et al.* have developed the time-stretch ADC (TS-ADC) and realized high sampling rate beyond

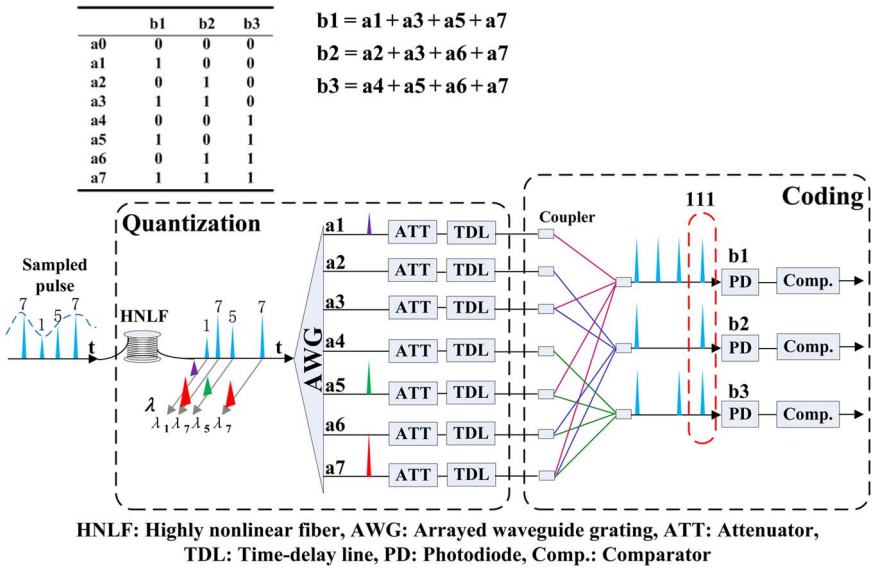

	b1	b2	b3
a0	0	0	0
a1	1	0	0
a2	0	1	0
a3	1	1	0
a4	0	0	1
a5	1	0	1
a6	0	1	1
a7	1	1	1

Fig. 1. Schematic diagram of a 3-bit AOADC based on SSFS technique.

100 GSa/s, but the quantization and coding modules still depend on the electrical processing [4], [5]. In order to achieve the high sampling rate and solve the bandwidth limitations of electronics, all-optical ADC (AOADC) with optical processing in both quantization and coding modules is the final objective [6]–[18]. AOADC based on the nonlinear optics effects has ultrafast response speed, which can realize the sampling rate transparency. Among the proposed schemes [10]–[15], the optical quantization based on soliton self-frequency shift (SSFS) effect is a promising candidate due to its spectral quantization characteristic. The quantized signals can be easily extracted with passive de-multiplexer. This scheme was first proposed by Chris Xu, and several improved results have been achieved by Konishi *et al.* [15]–[21]. A 6-bit quantization resolution has been realized by now using the SSFS effect, which is the state of the art in nonlinear AOADC [20]. However, the time-delay occurs inherently during the process of frequency shift. The amount of time-delay is proportional to the power of sampled pulses. Such a property has been utilized for the tunable slow light [22]. However, the non-synchronization of the quantized parallel pulse strings induced by the time-delay can directly result in the coding error. In Konishi's schemes [16], [17], the multiple time-delay lines (TDLs) related to the quantization resolution are used for the time-delay compensation, which increase the structure complexity of the AOADC greatly.

In this paper, we propose a novel lumped time-delay compensation scheme for the SSFS-based AOADC. By inserting a span of negative dispersion fiber (NDF) instead of the multiple TDLs after the quantization module, the time-delays of different quantized pulses are accurately compensated with a simple structure. Corresponding numerical analysis is demonstrated and discussed.

2. Principle of Operation

The schematic diagram of a nonlinear spectral quantization-based AOADC with 3-bit quantization resolution is shown in Fig. 1. The quantization and coding modules of such an AOADC are constructed by the highly nonlinear fiber (HNLF), arrayed waveguide grating (AWG), and other optical components. The discrete sampled pulses, which can be obtained with a high-repetition-rate optical pulse source by electro-optical modulation or four-wave mixing effect, are firstly delivered into a span of HNLF for quantization. After the transmission, different wavelength shift can be obtained due to the SSFS effect. In addition, different time-delays of quantized pulses occur simultaneously in time domain with the same law. The quantized pulses are separated with each other in an AWG and sent into the coding module. The coding is implemented by the optical interconnection (OI) module, which consists of several couplers, attenuators, TDLs, photodiodes, and comparators. The

multiple attenuators and TDLs are used to equalize the powers of the quantized pulses and compensate the different time-delays, respectively. The comparators after the PD array provide the final binary codes in a bit-parallel format. The law of the binary coding is according to the binary conversion table which is shown in the upper left part of Fig. 1.

The dynamic of the sampled pulses in the HNLF can be analyzed by solving the simplified Generalized Nonlinear Schrodinger Equation (GNLSE) described by

$$\frac{\partial A}{\partial z}+\frac{\alpha}{2}A+\frac{i\beta_2}{2}\frac{\partial^2 A}{\partial T^2}=i\gamma\left(|A|^2A-T_RA\frac{\partial|A|^2}{\partial T}\right) \tag{1}$$

where α, β_2, γ, and T_R are the attenuation parameter, second-order dispersion parameter, nonlinear coefficient, and Raman coefficient of the fiber, respectively. A is the complex amplitude of the optical field defined by

$$A(z,T)=\sqrt{\frac{E_0e^{-\alpha z}}{2\tau}}\mathrm{sech}\left(\frac{T-\Delta T}{\tau}\right)\exp\left[-i\Delta\Omega(T-\Delta T)-iC\frac{(T-\Delta T)^2}{2\tau^2}+i\phi\right] \tag{2}$$

where E_0 is the input pulse energy; $\Delta\Omega$ is the frequency shift of the pulse spectrum; τ, C, ΔT, and ϕ are the width, chirp, time-delay, and phase of the pulse, respectively. The third-order dispersion β_3 and self-steepening terms are omitted in Eq. (1), considering that the magnitude of β_3 is much smaller than β_2 and the carrier frequency is large enough. With the moment method (MOM), the frequency and temporal dynamic of the pulse can be obtained by [23], [24]

$$\Delta\Omega(L)=-\frac{8}{15}T_R\gamma P_0T_0\int_0^L\frac{1}{\tau^3(z)}dz \tag{3}$$

$$\Delta T(L)=\beta_2\int_0^L\Delta\Omega(z)dz=-\frac{8}{15}\beta_2T_R\gamma P_0T_0\int_0^L\left\{\int_0^z\frac{1}{\tau^3(z')}dz'\right\}dz \tag{4}$$

where L is the fiber length; P_0 and T_0 are the input peak power and width of the optical pulse, respectively. For the case of pure soliton, $\tau(z)$ is constant [23]. Eq. (3) shows that $\Delta\Omega$ is proportional to P_0, which can be beneficial to the spectral quantization operation. According to Eq. (4), it can be obtained

$$\Delta T\approx\Delta\Omega\cdot\beta_2\cdot L\approx\Delta\lambda\cdot D\cdot L=D\cdot L\cdot(\lambda_c-\lambda_0) \tag{5}$$

where $\Delta\lambda$ is the wavelength shift of the optical spectrum, $D=-2\pi c\beta_2/\lambda^2$ is the dispersion of fiber, λ_c is the central wavelength of optical pulse after quantization, and λ_0 is the input center wavelength. According to the proportional relation between ΔT and λ_c, the mechanism of the proposed lumped time-delay compensation is presented in Fig. 2.

The solid line is the time-delay curve with a slope of K_1, while the dash line is the time-delay compensation curve with a slope of K_2, $K_1=-K_2=(\Delta T_{\max}-\Delta T_{\min})/(\lambda_{\max}-\lambda_{\min})$. The dash line can be realized by using a span of fiber with the specific dispersion D'. According to the principle of dispersion compensation, it is easy to obtain $D'=-K_1/L'$. Here, L' is the length of the time-delay compensation fiber. This means that the time-delay can be compensated by a span of fiber with the flattened negative dispersion around $-K_1/L'$. For an AOADC with a certain resolution, the K_1 can be obtained prior. Thus, the length and dispersion of the time-delay compensation fiber can be appropriately selected.

3. Simulation and Discussion

According to the analysis above, the lumped time-delay compensation scheme is proposed, as shown in Fig. 3. A span of flattened NDF is inserted between the HNLF and the AWG to realize the

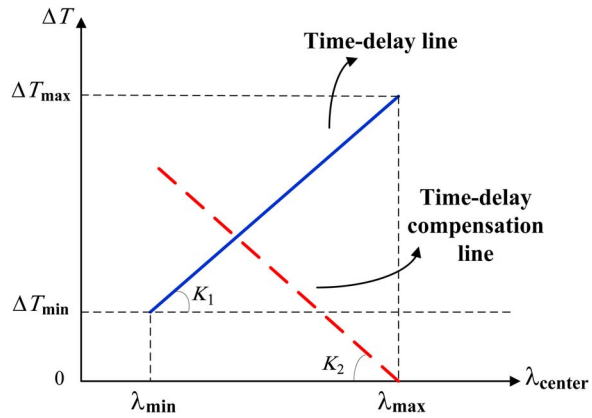

Fig. 2. The mechanism of the proposed lumped time-delay compensation.

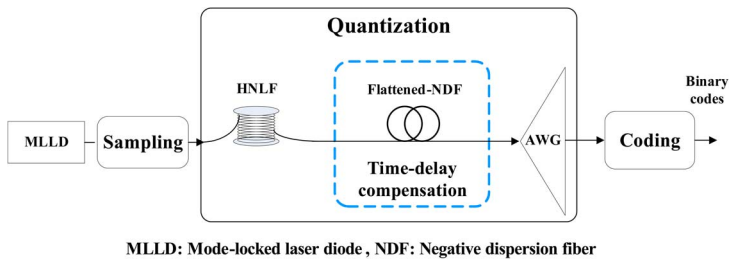

Fig. 3. Diagram of the lumped time-delay compensation scheme.

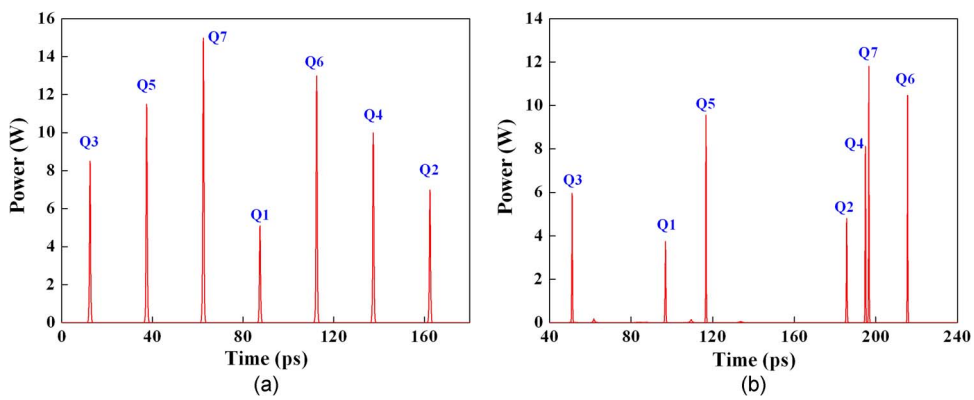

Fig. 4. (a) Seven sampled optical pulses and (b) delayed optical pulses after quantization.

lumped time-delay compensation, and thus, the multiple TDLs in Fig. 1 can be neglected. The simulation results can be obtained by solving the GNLSE with the split-step-Fourier method. The string of hyperbolic secant optical pulses with the FWHM of 0.53 ps, repetition of 40 GHz, and central wavelength of 1558 nm is launched by a mode-locked laser diode (MLLD). Via adjusting the peak powers of the pulses, the sampled pulses can be simulated. Seven optical pulses with the peak powers of 5.1 W, 7 W, 8.5 W, 10 W, 11.5 W, 13 W, and 15 W are generated, corresponding to seven quantization levels marked as $Q_1, Q_2, Q_3 \ldots, Q_7$, respectively. The temporal diagram is shown in Fig. 4(a).

The time interval of the pulses is 25 ps corresponding to the total sampling rate of 40 GSa/s. After transmitting in 1 km HNLF $(\gamma = 16\ \mathrm{W}^{-1}/\mathrm{km}, D = +3\ \mathrm{ps/nm/km}, \alpha = 0.9\ \mathrm{dB/km})$ for quantization,

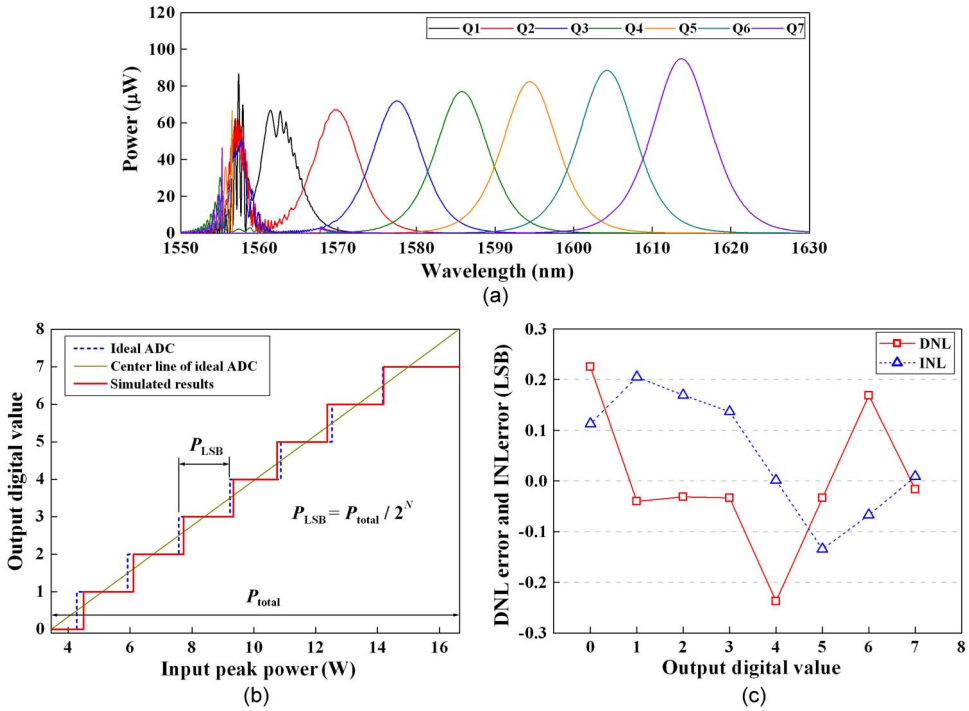

Fig. 5. (a) The spectral profiles of the quantized pulses. (b) Transfer function of the 3-bit AOADC. (c) Differential nonlinear error and integral nonlinear error.

the sampled pulses are respectively assigned to the specific wavelengths simultaneously with temporal delays. The delayed pulses are shown in Fig. 4(b). It can be obviously seen that the order of the pulses is disrupted, e.g., Q_5 and Q_7 with larger time-delays are exceeded by Q_1. This nonsynchronous issue can lead to the coding error in the final decision. Fig. 5(a) shows the spectral profiles of the quantized pulses. Seven-level wavelength shifts are generated corresponding to seven input powers. The quantization resolution N can be described as [16], [17]

$$N = \log_2\left(\frac{\lambda_{\text{shift}} + \Delta\lambda_{\text{FWHM}}}{\Delta\lambda_{\text{FWHM}}}\right) \tag{6}$$

where λ_{shift} and $\Delta\lambda_{\text{FWHM}}$ are the amount of center wavelength shift and the spectral width of the optical pulse after the SSFS, respectively. The λ_{shift} is 55 nm while the average $\Delta\lambda_{\text{FWHM}}$ is 7.25 nm, which results in $N = 3.1$ bit. It can be seen that the spectrum becomes overlapped with each other, which leads to the cross-talk between adjacent channels. Fortunately, the overlap points are all not higher than the FWHM level of the spectrum so that the cross-talk issue can be mitigated with the power equalization by the attenuator array and comparator decision. Fig. 5(b) shows the transfer function of the 3-bit AOADC. The transfer function is increasing monotonically without missing codes. The least significant bit (LSB) power P_{LSB} and the full-scale of power range P_{total} are 1.65 W and 13.2 W, respectively. Differential nonlinear (DNL) and integral nonlinear (INL) errors calculated from the transfer function are shown in Fig. 5(c). A peak DNL error of 0.24 LSB and a maximum INL error of 0.203 LSB are obtained, which ensures the resolution of the proposed 3-bit AOADC. The temporal profiles after the PD detection and the coding results with time-delay are shown in Fig. 6(a). Since the input optical pulses are "Q_3, Q_5, Q_7, Q_1, Q_6, Q_4, and Q_2," the correct codes should be "110 101 111 100 011 001 010." However, as shown in Fig. 6(a), the coding results become "110 000 100 101 000 010 111." The corresponding optical pulses become "Q_3, Q_0, Q_1, Q_5, Q_0, Q_2, and Q_7," which are inconsistent with the input ones. Thus, the time-delay compensation is quite necessary for ensuring the coding correctness.

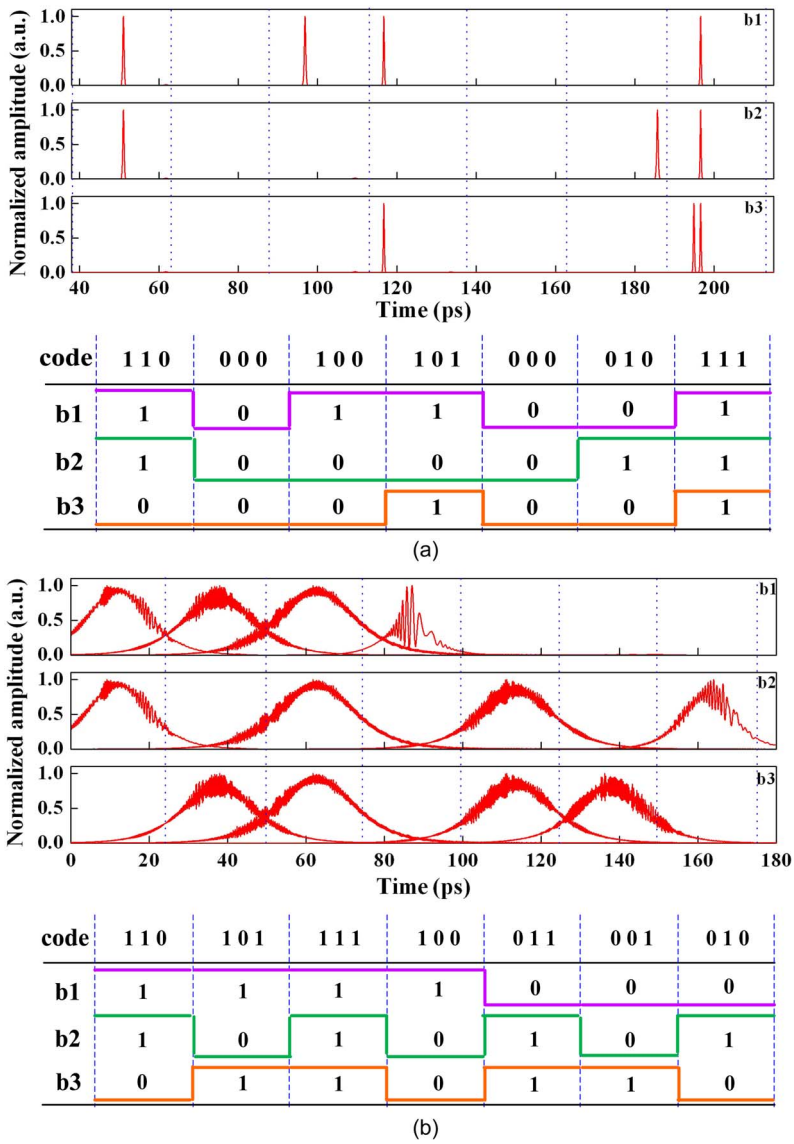

Fig. 6. Temporal profiles of the three quantization channels after PD detection and corresponding coding results (a) without time-delay compensation (b) with the proposed time-delay compensation.

In order to realize the proposed lumped time-delay compensation, a 10 m NDF with flattened dispersion in the wavelength range of 1558 to 1620 nm is inserted after the quantization module. Since the slope of the time-delay curve is $K_1 = 2.2$ ps/nm in this scheme, the dispersion value of -220 ps/nm/km is selected. The NDF can be fabricated with the multi-cladding design of dispersion compensation fiber, which is a mature technique at present. Correct binary codes are obtained with the proposed time-delay compensation, as shown in Fig. 6(b). However, because of the group-velocity dispersion effect of the NDF, the pulses after compensation are simultaneously broadened. This broadening effect can induce the limitation of the total sampling rate. If the FWHM of the broadened pulse is larger than the reciprocal of sampling rate, the broadened pulses will markedly interfere the decision of its adjacent pulses. This means that the wrong coding decision of "1" will replace the correct one of "0" in the final decision. It is evident that the slight interference has occurred in some decision window, as shown in Fig. 6(b). If the sampling rate is increased to a certain level, the wrong coding decision can be obtained. Considering the cases with different slopes K_1, the diagram of FWHM vs. central wavelength of the compensated pulses is shown in

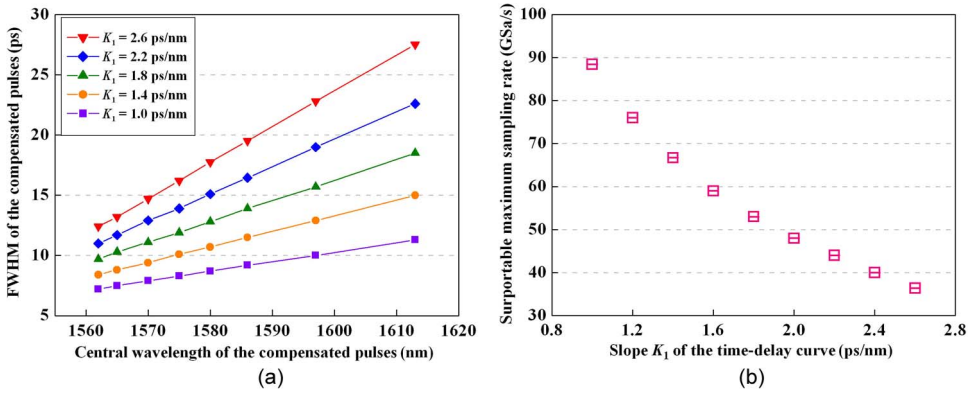

Fig. 7. (a) Curves of the FWHM vs. central wavelength of the compensated pulses (b) supportable sampling rate vs. slope K_1.

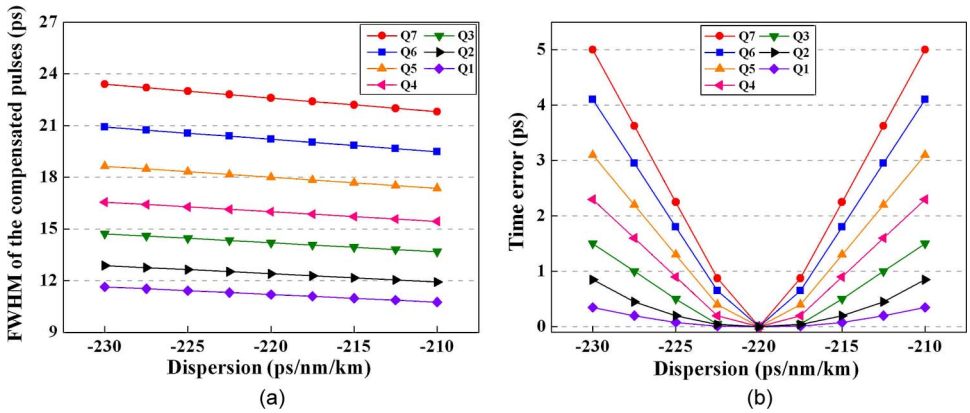

Fig. 8. The influences of the dispersion fluctuation, (a) FWHM of the compensated pulses vs. dispersion and (b) Time error vs. dispersion.

Fig. 7(a). K_1 is the slope of the time-delay curve, which is closely related to the amount of time-delay. With the increase of the central wavelength, the FWHM of the compensated pulse increases monotonically. Obviously, the pulse broadening effect can be suppressed by decreasing K_1. However, K_1 cannot be decreased without limitation because it is associated with the maximum wavelength shift. Enough wavelength shift must be obtained to ensure the quantization resolution according to Eq. (6). Since the central wavelengths are linearly related to the input sampled powers, the larger sampled power corresponds to the larger pulse broadening after the time-delay compensation. Therefore, the supportable sampling rate can be estimated by the broadened FWHM of the maximum sampled power. The estimated results are also shown in Fig. 7(b). For example, K_1 is 2.2 ps/nm and the maximum central wavelength is 1613 nm in our scheme. This means that the maximum FWHM of the compensated pulses is 22.6 ps, and the sampling rate should be no more than 44 GSa/s. If K_1 is reduced to 1 ps/nm with no impairments of the quantization resolution, a supportable sampling rate of 88 GSa/s can be obtained.

In practical fabrication, the dispersion of the flattened NDF cannot be a constant of -220 ps/nm/km. Considering the dispersion fluctuation within ± 10 ps/nm/km, the effect on the FWHM of the compensated pulses is shown in Fig. 8(a). With the decrease in dispersion, the FWHM of the seven compensated pulses all increase linearly. However, the variations are relative slight, which are all less than 1.6 ps. For example, the FWHM of Q_7 becomes 23.4 ps at the dispersion value of -230 ps/nm/km. According to the 22.6 ps at the dispersion value of -220 ps/nm/km, only 0.8 ps difference is obtained. Fig. 8(b) shows the diagram of time error vs. dispersion fluctuation. The time

error is defined as the difference between the time position of compensated pulses and the one of input pulses. If the time error is very large, the interference of pulses can still occur. It is evident that Q_7 has a relative large time error and its maximum is 5 ps. Considering both the pulse broadening and dispersion fluctuation issues, the maximum supportable sampling rate (MSSR) can be calculated by

$$MSSR = \frac{1}{2 \cdot (Time\text{-}error + FWHM_{\text{broadened}}/2)} \tag{7}$$

where *Time-error* and $FWHM_{\text{broadened}}$ are the amount of time error and the FWHM of the broadened pulses, respectively. Because the FWHM of Q_7 is less than 23.4 ps in this scheme, the pulse with broadening and time error will not severely interfere the decision of its adjacent pulses with the MSSR of 30 GSa/s. The same judgment can be made to the other coding pulses.

4. Conclusion

In summary, we proposed a novel lumped time-delay compensation scheme for simplifying the structure and ensuring the coding correctness of the SSFS-based AOADC. The 3-bit quantization resolution is illustrated in our analysis. The corresponding eight TDLs should be used for the time-delay compensation in the previous schemes. Using just a span of 10 m NDF instead, the construction of the AOADC can be simplified greatly with accurate time-delay compensation simultaneously. Actually, a potential 5-bit resolution can be realized with an additional spectral compression module since the total wavelength range is 55 nm [21]. The spectral compression can be realized by utilizing the dispersion-increasing fiber or the cascade structure of HNLF and SMF. Because 32 TDLs are needed for a 5-bit AOADC, the simplification effect can be more remarkable. Numerical results show that the delayed pulses can be accurately synchronized with the proposed lumped time-delay compensation scheme. A supportable sampling rate of 30 GSa/s is obtained when considering both the pulse broadening issue and dispersion fluctuation within $\pm$10 ps/nm/km. This means that the proposed scheme is very applicable to the bit rates of less than 2.5 Gb/s (12 samples per bit). In order to support higher sampling rate, our further work will be contracted on the matching pulse compression techniques in time domain.

References

[1] A. Khilo, S. J. Spector, and M. E. Grein, "Photonic ADC: overcoming the bottleneck of electronic jitter," *Opt. Exp.*, vol. 20, no. 4, pp. 4454–4469, Feb. 2012.
[2] G. C. Valley, "Photonic analog-to-digital converters," *Opt. Exp.*, vol. 15, no. 5, pp. 1955–1982, Mar. 2007.
[3] K. Xu, J. Niu, Y. T. Dai, X. Q. Sun, J. Dai, J. Wu, and J. T. Lin, "All-optical analog-to-digital conversion scheme based on Sagnac loop and balanced receivers," *Appl. Opt.*, vol. 50, no. 14, pp. 1995–2000, May 2011.
[4] Y. Han and B. Jalali, "Photonic time-stretched analog-to-digital converter: Fundamental concepts and practical considerations," *J. Lightwave Technol.*, vol. 21, no. 12, pp. 3085–3103, Dec. 2003.
[5] A. S. Bhushan, P. Kelkar, B. Jalali, O. Boyraz, and M. Islam, "130-GSa/s photonic analog-to-digital converter with time stretch preprocessor," *IEEE Photon. Technol. Lett.*, vol. 14, no. 5, pp. 684–686, May 2002.
[6] J. Stigwall and S. Galt, "Interferometric analog-to-digital conversion scheme," *IEEE Photon. Technol. Lett.*, vol. 17, no. 2, pp. 468–470, Feb. 2005.
[7] J. Stigwall and S. Galt, "Demonstration and analysis of a 40-Gigasample/s interferometric analog-to-digital converter," *J. Lightwave Technol.*, vol. 24, no. 3, pp. 1247–1256, Mar. 2006.
[8] Q. W. Wu, H. Zhang, M. Y. Yao, and W. Zhou, "All-optical analog-to-digital conversion based on polarization-differential interference and phase modulation," *IEEE Photon. Technol. Lett.*, vol. 19, no. 8, pp. 625–627, Apr. 2007.
[9] S. L. Wei, J. Wu, L. J. Zhao, C. Yao, C. Ji, D. Lu, X. L. Zhang, and Z. S. Yin, "Multimode interference coupler based photonic analog-to-digital conversion scheme," *Opt. Lett.*, vol. 37, no. 17, pp. 3699–3701, Sep. 2012.
[10] X. Chris and X. Liu, "Photonic analog-to-digital converter using soliton self-frequency shift and interleaving spectral filters," *Opt. Lett.*, vol. 28, no. 12, pp. 986–988, Jun. 2003.
[11] K. Ikeda, J. Mohammad, S. Namiki, and K. I. Kitayama, "Optical quantizing and coding for ultrafast A/D conversion using nonlinear fiber-optic switches based on Sagnac interferometer," *Opt. Exp.*, vol. 13, no. 11, pp. 4296–4302, May 2005.
[12] S. I. Oda and A. Maruta, "A novel quantization scheme by slicing supercontinuum spectrum for all-optical analog-to-digital conversion," *IEEE Photon. Technol. Lett.*, vol. 17, no. 467, pp. 465–467, Feb. 2005.
[13] Y. Miyoshi, K. Ikeda, H. Tobioka, T. Inoue, S. Namiki, and K. I. Kitayama, "All-optical analog-to-digital conversion using split-and-delay technique," *J. Lightwave Technol.*, vol. 25, no. 6, pp. 1339–1347, Jun. 2007.

[14] Y. Miyoshi, S. Takagi, S. Namiki, and K. I. Kitayama, "Multiperiod PM-NOLM with dynamic counter-propagating effects compensation for 5-bit all-optical analog-to-digital conversion and its performance evaluations," *J. Lightwave Technol.*, vol. 28, no. 4, pp. 415–422, Feb. 2010.
[15] T. Nishitani, T. Konishi, and K. Itoh, "Integration of a proposed all-optical analog-to-digital converter using self-frequency shifting in fiber and a pulse-shaping technique," *Opt. Rev.*, vol. 12, no. 3, pp. 237–241, May 2005.
[16] T. Nishitani, T. Konishi, and K. Itoh, "Optical coding scheme using optical interconnection for high sampling rate and high resolution photonic analog-to-digital conversion," *Opt. Exp.*, vol. 15, no. 24, pp. 15 812–15 817, Nov. 2007.
[17] T. Nishitani, T. Konishi, and K. Itoh, "Resolution improvement of all-optical analog-to-digital conversion employing self-frequency shift and self-phase-modulation-induced spectral compression," *IEEE J. Sel. Topics Quantum Electron.*, vol. 14, no. 3, pp. 724–732, May/Jun. 2008.
[18] T. Satoh, K. Takahashi, H. Matsui, K. Itoh, and T. Konishi, "10-GS/s 5-bit real-time optical quantization for photonic analog-to-digital conversion," *IEEE Photon. Technol. Lett.*, vol. 24, no. 10, pp. 830–832, May 2012.
[19] C. Xu and X. Liu, "Photonic analog-to-digital converter using soliton self-frequency shift and interleaving spectral filters," *Opt. Lett.*, vol. 28, no. 12, pp. 986–988, Jun. 2003.
[20] T. Konishi, K. Takahashi, H. Matsui, and T. Satoh, "Optical quantization for 6 bit photonic A/D conversion," in *Proc. Int. Conf. Transp. Opt. Netw.*, Coventry, U.K., Jul. 2, 2012, pp. 1–3.
[21] T. Konishi, K. Takahashi, H. Matsui, T. Satoh, and K. Itoh, "Five-bit parallel operation of optical quantization and coding for photonic analog-to-digital conversion," *Opt. Exp.*, vol. 19, no. 17, pp. 16 106–16 114, Aug. 2011.
[22] S. Oda and A. Maruta, "All-optical tunable delay line based on soliton self-frequency shift and filtering broadened spectrum due to self-phase modulation," *Opt. Exp.*, vol. 14, no. 17, pp. 7895–7902, Aug. 2006.
[23] G. P. Agrawal, *Nonlinear Fiber Optics*, 4th ed. San Diego, CA, USA: Academic, 2007.
[24] R. Liang, "All-optical quantization based on the Raman self-frequency shift and spectral compression," Ph.D. dissertation, Univ. Electron. Sci. Technol. China, Chengdu, China, 2010.